

Turbulent Spatial Structure in a Drag-Reducing Flow with Surfactant Additives Investigated by PIV System

Y. Kawaguchi and Z. Feng

*Mechanical Engineering Laboratory, AIST METI, 1-2 Namiki Tsukuba, 305-8564 Japan

The turbulent frictional drag of water can be reduced dramatically by adding small amounts of drag-reducing materials, such as polymers or surfactants. As the amount of percentage drag reduction easily reaches 80%, this technique is thought to be the most practical method to reduce turbulence frictional drag. In this work, a double pulse PIV system was used to clarify the spatial velocity distribution of surfactant solution flow in a two-dimensional channel of height 40mm, width 500mm and length 6m. A type of cationic surfactant CTAC ($C_{16}H_{33}N(CH_3)_3Cl$) mixed with same weight of counter-ion material NaSal (HOC_6H_4COONa) was used as a drag-reducing additives to water at a mass concentration of 40ppm. Instantaneous velocity distribution taken by PIV was examined to clarify the effect of surfactant additives as well as Reynolds number dependency of drag reducing flow.

The following conclusions were drawn from the present study.

1. Figure 1 shows the velocity field with and without surfactant additives. Each figure shows the x-y plane along the centerline of the channel. As seen in Fig. 1a, the mean velocity distribution taken in drag-reducing flow differs from turbulent one in water flow without additives. Investigation of instantaneous velocity distribution shows that random vortex motion disappears. An intermittent change of flow such as turbulent slug was not observed in present study.
2. Figure 1b shows the structure of penetration of low speed fluid into high-speed region, which is one of the important events of turbulence energy production and turbulent mixing. Although this structure is commonly observed in water flow, it was not found in drag-reducing flow under the same Reynolds number (see Fig.1a). The strong vorticity fluctuation near the wall also disappears in drag-reducing flow.
3. As the Reynolds number increases and enters into "post DR region" where Reynolds number exceeds critical value, the drag-reducing flow starts to become unstable and the PIV picture shows an appearance of turbulent motion near the wall.

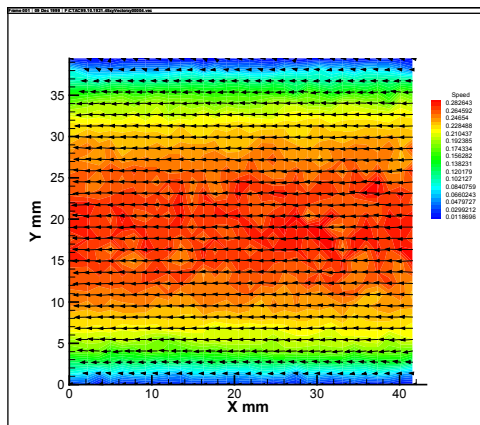


Fig. 1a. Instantaneous velocity distribution in drag-reducing flow (CTAC 40ppm) at $Re=21000$

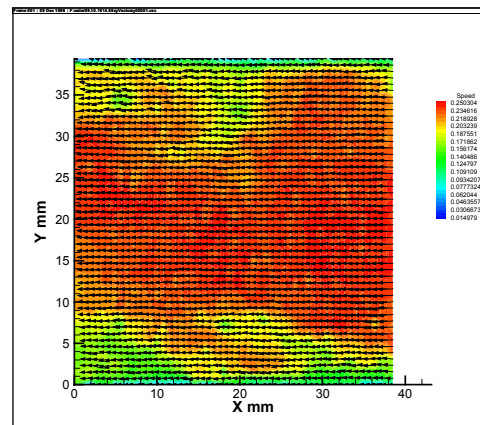


Fig. 1b. Instantaneous velocity distribution in water flow (CTAC 0ppm) at $Re=21000$

The figure covers the full channel height. The upper and lower limit of the figure shows the top and bottom surfaces of the channel respectively. The main flow direction is from right to left. The contours are colored according to the instantaneous velocity

1. Introduction

Since the discovery of Tom's effect (Mysels, 1949, Toms, 1948), the reduction of turbulent friction between a solid surface and fluid by adding drag-reducing materials has received increasing attention for saving the pumping power in fluid transportation. Polymers were initially used as drag-reducing additives for turbulent water flow to reduce the frictional drag by up to 80%. However, polymer solutions are strongly affected by mechanical degradation, which may result in shorter lifetime of drag reduction effectiveness. Surfactants were found in the last two decades also to reduce the frictional drag by 70% to 80% but to be less affected by mechanical degradation (Ohlendorf et al. 1986, Bewersdorff et al., 1988). Therefore, surfactants are now being considered as practical drag-reducing additives.

One successful application of drag reduction by adding polymers was in the Trans-Alaska Pipeline, where the target discharge of one million barrels per day was obtained without having to construct additional pumping stations (Burger et al., 1982). A more recent application of the drag-reducing additives is to reduce the pumping power in district heating and cooling systems where cationic surfactants are used in closed circuits (Gyr and Bewersdorff, 1995, Gasljevic and Matthys, 1997, Pollert et al., 1994). Although the environmental contamination arising from the minor toxic effect of surfactants may restrict their practical application in industry, for a closed circuit the effect on the environment can be minimized to an acceptable level.

The authors are continuing experimental studies on drag reduction phenomena in order to optimize district heating/cooling systems (Kawaguchi et al. 1996a, 1996b, 1997a, 1997b, Li et al, 2000). Kawaguchi et al. (1996a) carried out an investigation to see how the turbulent characteristics in a two-dimensional channel are modified by surfactant additives by using a two-component LDV system, and discussed the effect of surfactant concentration and Reynolds number. They found that the two components of turbulent intensity were suppressed but have a finite value. Surprisingly, Reynolds shear stress disappears in fully drag-reducing flow as a result of the de-correlation of the two components of velocity fluctuation.

As the surfactant solution flow exhibits a complicated dynamical and thermal response, hot-film or other intrusive methods are unsuitable for measuring flow characteristics. Although the LDV allows us to make accurate measurements, measurements is limited to only one point at a time. Therefore, little information on the spatial structure such as length scale of turbulence can be revealed by LDV. In contrast, PIV gives spatial information instantaneously. For this reason, PIV was employed to investigate the structure of drag-reducing flow in this paper.

2. Experimental Apparatus and Procedure

2.1 Water Channel

The present experiments were carried out in a closed liquid flow loop, which is shown in Figures 2a and 2b. The system consists of a reservoir tank (2.0 m³), a pump, a settling chamber equipped with a nozzle, a two-dimensional channel, a diffuser and an electro-magnetic flow meter. The test section is 40mm high (H), 500mm wide (W) and 6m long (inside measurements). Most of the test section was made of transparent acrylic resin having thickness of 20mm. The surfactant aqueous solution is circulated by the pump and supplied to the settling chamber, which is equipped with a perforated pipe, stainless steel mesh and 1/12.5 contraction nozzle. At the entrance of test section, a honeycomb of 150mm length having 10mm by 10mm rectangular openings was used to remove large eddies. The PIV measurement position (L) is 3000mm ($=75H$) downstream from the inlet of the test section. For measurements of pressure drop, a high-precision differential pressure meter was used. The reading provided by the flow meter and the flow rate calculated from the velocity profile measured by LDV coincided within 3%.

2.2 PIV system

The PIV measurement system consists of a double pulse laser, laser sheet optics, CCD camera, timing circuit, PC and software. The double pulse laser, (New wave Research Co. Ltd., MiniLase – II/20Hz) is a combination of a

pair of Nd-YAG lasers with each having an output of 25mJ/pulse and repetition rate of 20Hz. By changing the combination of cylindrical lens, the laser sheet thickness can be modified in the range of 0.14mm to 0.6mm and spread angle in the range of 4.3 deg to 13.3 deg. The timing circuit (TSI Model 610032) communicates with the CCD camera and computer, and generates pulses to control the double pulse laser. The time duration of laser pulses was adjusted to give reasonable vector images. The interline CCD camera (PIVCAM 10-30, TSI Model 630046) used has a resolution of 1008 by 1018 pixels and can transfer images to the computer at the rate of 30 frames per second.

A personal computer (Pentium II, 400MHz) equipped with image grabber board (TSI Model 600067) was used to control the whole system, picture frame acquisition and data processing using TSI's Insight ver. 2.01 software. As the generation of error vector caused by imperfect condition of the optical system or software was unavoidable, a special Fortran program was written for eliminating the error vectors and performing statistical calculation based

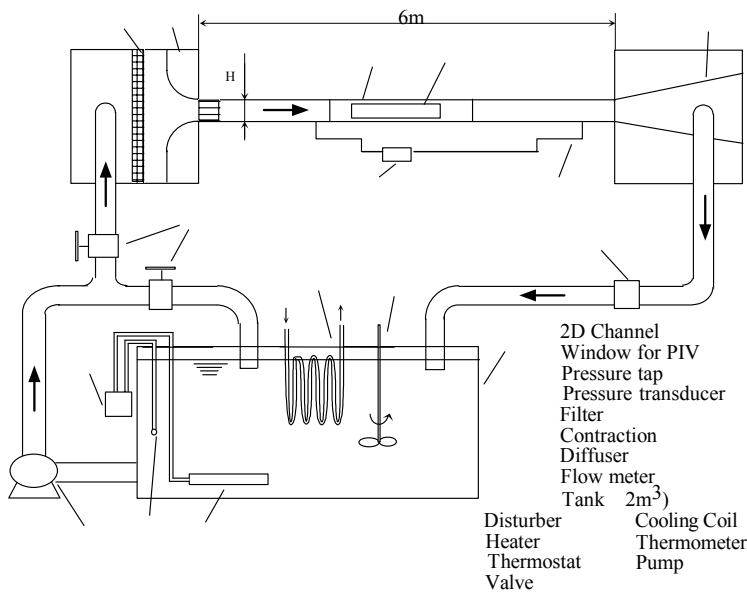


Fig. 2a. Schematic diagram of two dimensional water channel Inner height: $H=40\text{mm}$, width: $W=500\text{mm}$. All the measurements were made at $x=3000\text{mm}$.

Fig. 2b. Picture of the channel Seen from contraction. Major parts are made of transparent acrylic resin.

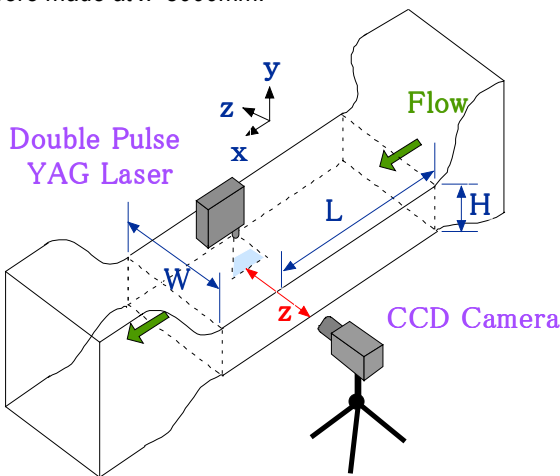


Fig.3. Schematic view of PIV arrangement CCD Camera detects instantaneous velocity distribution in x - y plane including full height of the channel ($40 \times 40\text{mm}$)

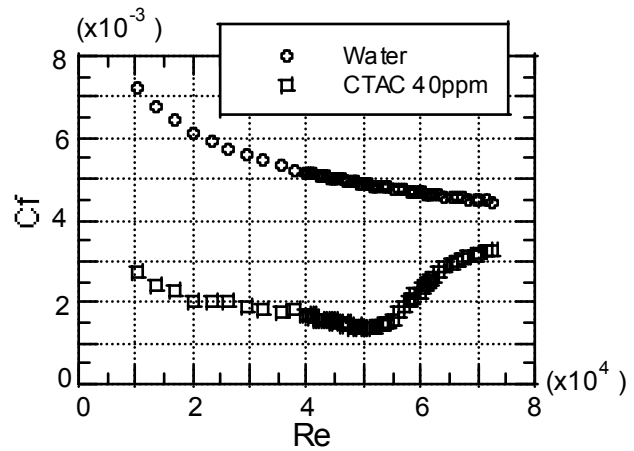


Fig. 4. Friction factor versus Re
 Re_c : Critical Reynolds number. I: complete DR flow
 II: Post DR flow

on the acquired vector distribution. The arrangement of the water channel and PIV system are shown in Fig. 3. Cartesian coordinate are also shown in the diagram. According to the common usage, x , y and z coordinates is aligned to the streamwise, normal to the bottom wall and spanwise directions respectively. At the location of the measurements, the channel is equipped with two circular glass windows having aperture of 150mm on the top and bottom walls of the channel. Another two glass windows, each with a rectangular opening of 200mm in the x -direction by 60mm in the y -direction, are installed on both sides of the channel. PIV image in the x - y plane are taken through the rectangular window from the z -direction. To allow this, a laser sheet aligned in the x - y plane is emitted from the top of the channel through the circular window. Most of the picture frames (40mm by 34mm) were taken to cover full height of the channel. In most of the experiments, a series of 48 frames at the rate of 30 frames per second was taken. This means velocity field was recorded in 15 Hz. Fine particle of aluminum oxide were used for scattering particles, with nominal particle diameter of 5 μ m. The concentration was carefully controlled to show clear PIV pictures.

2.3 Surfactant solution

The surfactant solution used in this study was cetyltrimethyl ammonium chloride (CTAC), which has the chemical formula of $C_{16}H_{33}N(CH_3)_3Cl$, dissolved in tap water. CTAC is a cationic surfactant that is known to be very effective for drag reduction when accompanied with suitable counter ions. Cationic surfactants are less affected by calcium or sodium ions naturally found in tap water. This is the reason why cationic surfactants combined with a counter ion such as sodium salicylate (NaSal, HOC_6H_4COONa) are frequently used in the basic studies or application to district heating and cooling systems.

For the surfactant drag-reducing additives, the rod-like micelle structure is thought to be the key to give complicated rheological fluid properties including viscoelasticity. NaSal acts to reduce ion radius of CTAC to deform micellar shape from globular to rod like. In this experiment, same weight concentration of NaSal is always included in the CTAC solution. For the sake of simplicity, the solution of surfactant is designated by the surfactant concentration.

Prior to the channel experiment, viscosity of the solution was measured by a rheometer with double wall Couette geometry (Rheometric Scientific F.E. Ltd., ARES 100FRTN1). At concentrations of 30ppm and 100ppm, the shear viscosity of the solution at a shear rate of 200 s^{-1} in 25 deg C was 0.82 and 0.97 mPas respectively, and showed no stress thinning in the range of 10 s^{-1} to 300 s^{-1} .

3. Results and Discussion

3.1 effect of surfactant additives on friction factor and local mean velocity

The friction factor experimentally determined for water with and without surfactant additives is presented in Fig. 4. Friction factors were obtained from static pressure distribution measurements along the channel. The Reynolds number was estimated from bulk mean velocity U_b , channel height H and solvent kinematic viscosity ν_0 . The friction factor for water varies smoothly and obeys Dean's (1978) experimental formula for channel flow of Newtonian fluid. In contrast, the friction factor of the surfactant solution changes in a complicated way. It is observed that friction factor rises at $Re=51000$. This critical Reynolds number separates two regimes, namely "complete DR flow" and "post DR flow", as previously called by Kawaguchi et al. (1997b). The largest percentage of drag reduction in this experiment was around 60%.

The mean velocity profile was determined based on the instantaneous velocity distribution taken by PIV. In each frame k , two components of velocity U and V at grid points x_i and y_j can be obtained. As location of grid point in each frame is fixed, we can define local mean velocity as the ensemble average through x_i and frame number k as follows.

$$\bar{U}(y_j) = \frac{1}{KI} \sum_{k=1}^K \sum_{i=1}^I U(x_i, y_j, k) \quad (1)$$

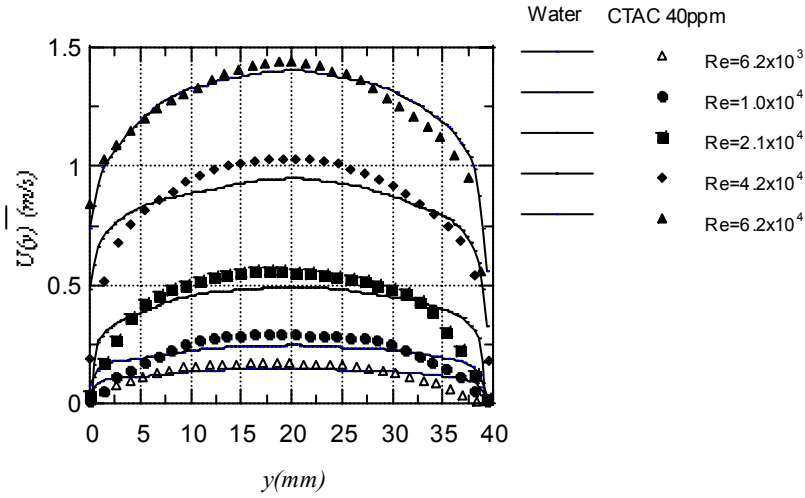


Fig. 5. Mean velocity profiles at various Reynolds numbers measured by PIV (lines: water, symbols: surfactant 40ppm)

In the typical case, grid number I and J in a frame was 50, frame number was 48. The local mean velocity was calculated based on 2400 data of instantaneous velocity measured at each y_j .

The obtained mean velocity profiles with surfactant for various Reynolds numbers are shown in Fig. 5, where lines represent the velocity profiles for water at each Reynolds number. It is well known that the velocity profiles for water is roughly correlated by $1/n$ power law. In this Reynolds number range, mean velocity near the centerline of the channel becomes flat and velocity gradient near the wall is large. In contrast with this, velocity profiles for surfactant solution show steeper peak near the centerline, which the mean velocity gradient near the wall of surfactant solution is lower than that of the water flow. This finding corresponds to the result obtained by LDV (Kawaguchi et al. 1996a) that the velocity profile of drag-reducing flow approaches to but does not coincide to laminar-like velocity profile.

3.2 Effect of surfactant additives to instantaneous velocity distribution

At the beginning, instantaneous velocity distribution for water flow at $Re=21000$ is discussed. Figure 6 shows a vector (Fig. 6a) and contour (Fig. 6b) expression of spatial velocity distribution taken by PIV. In these figures, main flow direction is from left to right and frame covers the height of the channel. In Fig. 6a, bulk mean velocity U_b was subtracted from all the vectors to see the vortex motion moving with U_b . This expression can be thought to give picture taken by a camera moving with the flow. So, the wall looks to move downstream direction at the speed of U_b .

Figure 6a shows a velocity field composed of irregular direction as well as irregular magnitude of the velocity vectors. Generally, velocity vectors head to right at the core region where y falls within 10mm to 30mm. In contrast with this, vectors within 5mm from the wall head to the left. Between these regions, the rotational eddy motion is clearly seen. The center location, size and magnitude of eddies are irregular. Figure 6b shows the contour map based on the magnitude of velocity, where random pattern of complicated ridge, valley and peaks can be seen in the middle of the channel. This means large velocity fluctuation in time and space occupies this field. In the region closer than 3mm from the wall, contour lines are closely distributed. This comes from the large velocity gradient near the wall, which is commonly seen in turbulent wall flow.

Figure 1b gives basically the same information as Fig. 6. One interesting finding from the colored contour is the existence of the acceleration or deceleration fronts near the wall. The acceleration front starts from the location of $(x, y)=(15\text{mm}, 1\text{mm})$ and reaches to $(5\text{mm}, 7\text{mm})$. This front inclines downward and has an angle of about 30 deg

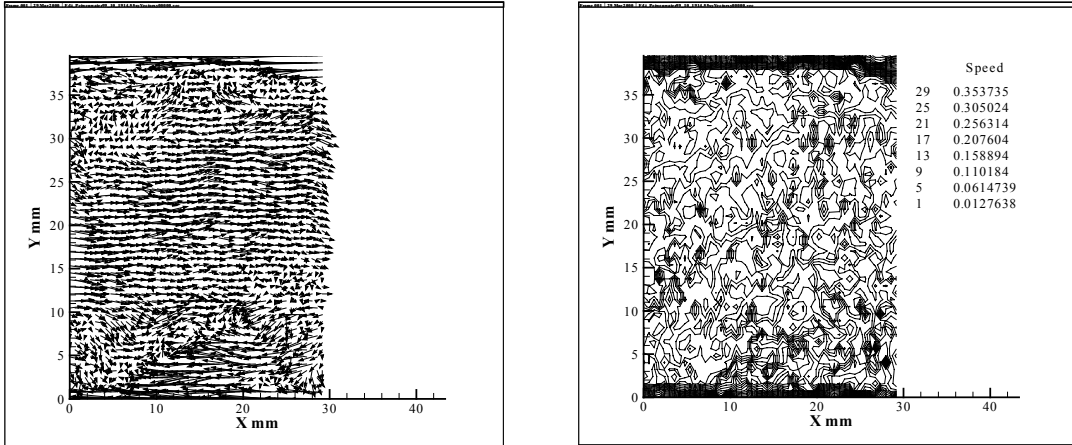


Fig. 6. Instantaneous velocity distribution in water (CTAC 0ppm), $Re=21000$

Fig. 6a (Left): Velocity vector. Bulk mean velocity U_b was subtracted from all the velocity

Fig. 6b (Right): Contour according to velocity magnitude.

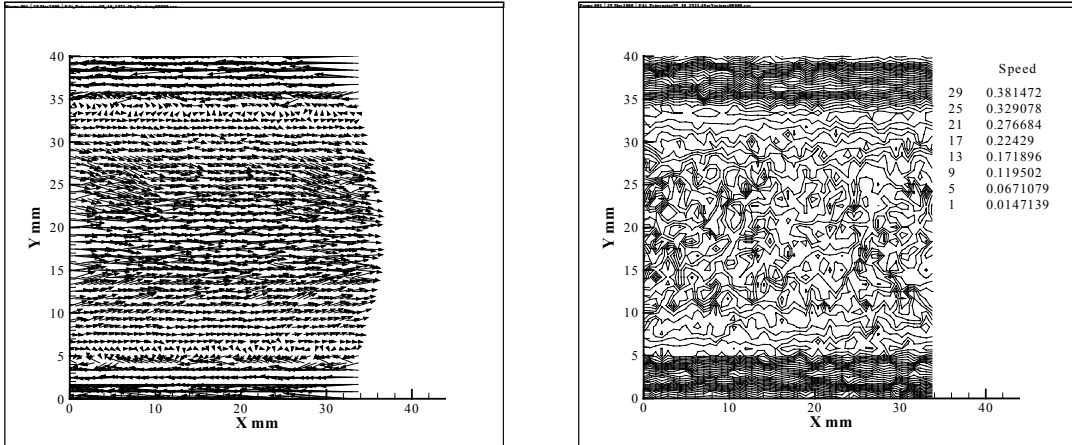


Fig. 7. Instantaneous velocity distribution in surfactant solution (CTAC40ppm), $Re=21000$

Fig. 7a (Left): Velocity vector. Bulk mean velocity U_b was subtracted from all the velocity

Fig. 7b (Right): Contour according to velocity magnitude.

Each figure covers the full channel height. The upper and lower limit of the figure shows the top and bottom surfaces of the channel respectively. The main flow direction is from left to right.

to the wall, noting that the mean flow direction in Fig. 1 is from right to left. Another acceleration front appears at the location between (35mm, 3mm) and (23mm, 7mm). Deceleration front is not clear but can be seen between (27mm, 2mm) to (20mm, 7mm). These acceleration or deceleration fronts are characteristic features of the nearwall turbulence. The turbulent structure accompanied with rapid acceleration or deceleration was investigated by VITA method applied to hot wire record (Blackwelder and Kaplan, 1976, Johansson and Alfredsson, 1982). A study on spatial structure relating to turbulence control was also made based on the hot wire array probe (Kawaguchi et al., 1983).

Figure 7 shows the velocity field obtained with surfactant solution flow, where Reynolds number is 21000 and equal to the case in Fig. 6. Two figures in Fig. 7 are vector and contour expressions of the spatial velocity distribution, respectively. Bulk mean velocity U_b was subtracted from the vectors and show in Fig. 7a to see the vortex motion moving with U_b . Tilting angle of mean flow and each velocity vector are not always zero but much smaller than that in Fig. 6a. A weakly accelerated region can be seen in Fig. 7a at $(x, y)=(7mm, 25mm)$ and $(30mm, 25mm)$ but vortex motion cannot be clearly detected from this figure. Kawaguchi et al., (1996a) found

that the dye streak in water is diffused by eddies with various sizes. But the dye streak in drag-reducing flow is much stable and slowly curved and it suggests diminish of random motion of eddies. The present result given by PIV corresponds to our previous flow visualization study.

Figure 7b also shows complicated ridge and valley pattern in the core region at $y=10\text{mm}$ and 30mm . In the region closing to the wall within 10mm , the contour lines run approximately parallel to the wall and their spaces are wider than the case in water flow shown in Fig. 6b. This difference comes from the thickened shear layer and the smaller velocity gradient near the wall. The reason and mechanism of drag reduction by additives are still under discussion due to the limit of experimental and analytical data. In addition to this, turbulence production is essentially a recurring process. We can observe the weak turbulence intensity in drag reducing flow and this suggests low production rate. Production rate of turbulence sometimes expressed as Reynolds shear stress multiplied by mean velocity gradient. These two terms can have small values in weakened turbulence intensity. Therefore, we encounter difficulties to isolate the reason for lower production rate from simple observation.

According to Kawaguchi et al. (1996a), in fully drag reducing flow, turbulent intensities of both u' and v' components are suppressed but have finite value. The suppression ratio of y -directional component is much larger than the ratio of x -directional component. An astonishing fact is that the Reynolds shear stress disappears in whole range of the channel. Therefore, correlation factor of two velocity components R_{uv} is completely zero in spite of the presence of u' and v' . Kawaguchi et al. (1997b) also found that coherent structure detected by quadrant analysis shows no distinguished contribution from sweep or ejection. In other words, contribution from wallward and outward interaction are comparable to sweep and ejection.

In Newtonian fluid flow such as water, two components of velocity fluctuation usually have negative correlation in shear layer. The idea of mixing length hypothesis is widely accepted to give a good approximation in such case. This idea contains random movement of fluid particles, and complete mixing after certain time period. De-correlation of turbulence components in drag-reducing shear flow suggests that some of the idea in mixing length theory is unsuitable for non-Newtonian fluid. The free movements of fluid particles are inhibited in drag reducing state. Some inhibition force is required but shear viscosity cannot stand because such a phenomenon is observed in the large Reynolds number.

The investigations are still going on but force coming from extensional viscosity can be one of the candidates. Trouton ratio is defined as the ratio of the extensional viscosity and shear viscosity. All the low molecular weight fluid has a Trouton ratio of 3 but some polymeric liquid exhibits much larger values such as 10000. Although all the drag-reducing fluid have complicated Rheological properties, large Trouton ratio is commonly found in drag-reducing fluid including dilute surfactant solution used in the present study. If we suppose the high extensional viscosity, stretching motion of vortex will be inhibited and production rate will be suppressed. At the same time, movement of the fluid must overcome the strong stretching resistance and discrepancy from the mixing length hypothesis becomes large. Another aspect of drag reduction flow is inhomogeneous turbulence suppression, which means y -directional components v' are much suppressed than x -directional one, u' . This can be also explained by large extensional viscosity. Due to the redistribution process, the excess energy of one components, such as u' is shared to another components v' and w' . In the case of drag-reducing flow, x -directional component does not redistributed to y or x -directional components. This may explain the observation that v' is much suppressed than u' in drag-reducing flow. This inhomogeneous suppression comes from the inhibition of energy transfer from u' to v' by large resistance of eddy stretching.

As above qualitative explanation contains hypothetical idea, further investigations and effort to quantitative estimation are necessary in the future. One of the projects would be the accurate characterization of the drag reducing solution by sensitive Rheometer. The other one may be the direct Navier-Stokes simulation of non-Newtonian fluid turbulence containing reasonable constitutive equation.

One of the advantages of PIV measurements is that it can offer information of vorticity based on the spatial distribution of velocity. In wall turbulence, velocity gradient has large value near the wall. Therefore, local mean velocity was subtracted from the instantaneous velocity to eliminated the contribution of mean velocity gradient to

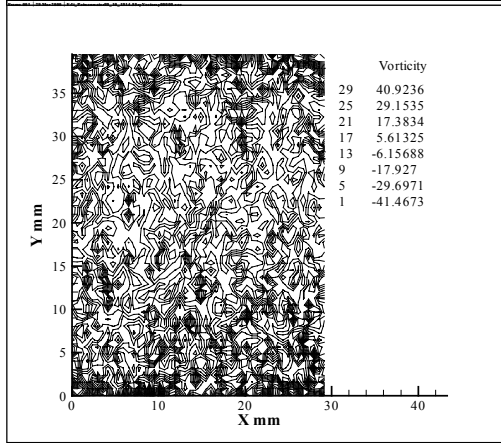


Fig. 8a. Vorticity fluctuation distribution in water flow (CTAC 0ppm) at $Re=21000$, $-41.5s^{-1} < \omega_z' < 40.9 s^{-1}$

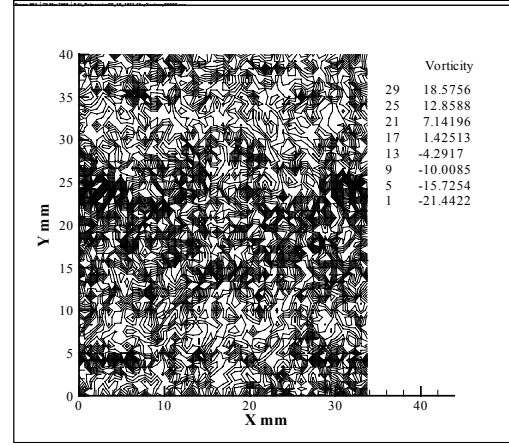


Fig. 8a. Vorticity fluctuation distribution in drag-reducing flow (CTAC 40ppm) at $Re=21000$, $-21.4 s^{-1} < \omega_z' < 18.5 s^{-1}$

Contour lines in each figure are drawn at the class of 8 levels between minimum and maximum value in each frame. The main flow direction is from left to right

vorticity. Vorticity fluctuation ω_z' is defined as follows.

$$\omega_z'(x_i, y_j) = \frac{1}{2} \left[\frac{\partial V(x_i, y_j)}{\partial x_i} - \frac{\partial}{\partial y_j} \{U(x_i, y_j) - \bar{U}(y_j)\} \right] \quad (2)$$

Figures 8a and 8b show comparison of vorticity fluctuation with and without surfactant additives. Note that contour lines are drawn to divide the range defined by minimum and maximum values appearing in the frame. These values are designated under each figure. As shown in Fig. 8a, large positive and negative vorticities were observed near the wall and its spatial scale is small in the case of water. In comparison with this, surfactant additives suppress violent vortical motion. Vorticity fluctuation is relatively weak and evenly distributed and its size is large.

3.3 Effect of Reynolds number in drag reducing flow

Kawaguchi et al. (1997b) conducted measurements of turbulence by LDV in the same channel and examined the Reynolds number dependency of the flow. They divided the Reynolds number range into four regions according to the friction factor behavior. In the range of large drag reduction, where we are most interested, was separated into two regimes as "complete DR region" and "post DR region" by critical Reynolds number. Large drag reduction rate and low turbulence intensity characterize the complete DR region. Reynolds shear stress was zero and it comes from the de-correlation of two components of velocity fluctuation. Along with the increasing of Reynolds number, frictional factor gradually increases and flow approaches to turbulent mode in Newtonian fluid. One interesting finding by Kawaguchi et al. (1997b) is that in post DR region, de-correlation of two components of velocity fluctuation, which is a key phenomena in drag-reduction, disappears. In post DR region, the state of flow is a kind of mixture of drag reducing state and normal turbulent state because the frictional drag and turbulence intensity comes into the midway of two states. But the correlation coefficient of two components of velocity fluctuation takes comparable value with that of normal turbulent state.

Figures 9 shows the velocity distribution in drag reducing flow at different Reynolds numbers. According to the classification in Fig. 4, cases for Figs. 9a to 9d belongs to the complete DR flow and other two belongs to the post DR flow. It can be observed that the flow starts to be unstable at $Re=42000$. At $Re=52000$ and 62000 , the figures contain typical motion in turbulent flow of Newtonian fluid. The penetration of low speed fluid into high speed flow, and the acceleration front can be seen in Figs. 9e and 9f. According to these figures, flow state in post DR

flow can be thought to be a combination of drag reducing flow in core region and turbulent flow near the wall. Controlling drag reduction, which means temporal termination of drag reduction, is also important issue for industrial application of this technology (Li et al., 2000). The finding of such a combination is interesting from the view of controlling drag reduction phenomena. The velocity fluctuation observed near the wall has similar characteristics as that of in ordinary turbulence because the correlation between two velocity components has large negative value (Kawaguchi et al., 1997b). But at $Re=62000$, the occurrence of such a motion is still insufficient to recover the turbulent transport. The drag reduction rate is still large and have a value of 30% (Fig.4) and mean velocity profile is different from that of water when this Reynolds number, as seen in Fig. 5. Therefore, giving disturbance in the near wall region by some obstacle is not a good method if the core region remains drag-reducing state. Kawaguchi et al. (1996b) tried to give disturbance by heater strip on the channel wall. The idea comes from the micellar structure destruction by high temperature at the heater. Slightly enhanced Reynolds shear stress was observed but heat transfer enhancement or increase of frictional drag was not achieved. Kawaguchi et al. (1997a) also investigated the thermal boundary layer in drag reducing flow and found double diffusivity layers. This can be explained by the present observation that flow can be unstable in near wall region but still covered by stable drag-reducing flow in outer layer.

4. Conclusions

The following conclusions were drawn from the present study.

1. The instantaneous velocity distribution taken in drag-reducing flow differs from that in water flow without additives. Investigation of instantaneous velocity distribution shows that random vortex motion

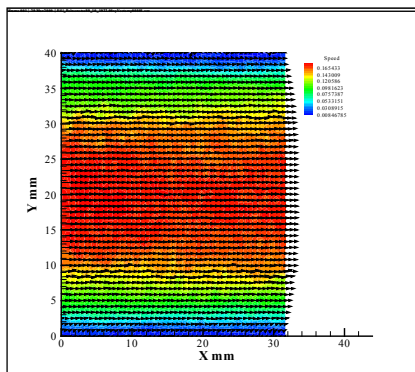


Fig. 9a. $Re=6200$

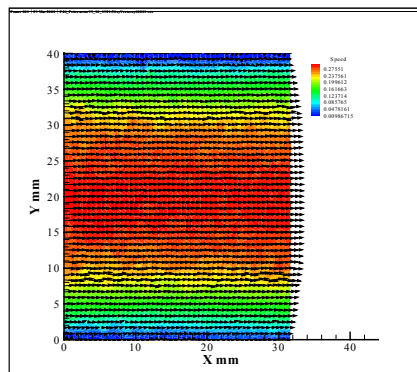


Fig. 9b. $Re=10000$

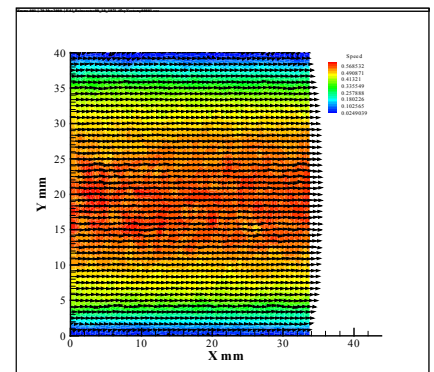


Fig. 9c. $Re=21000$

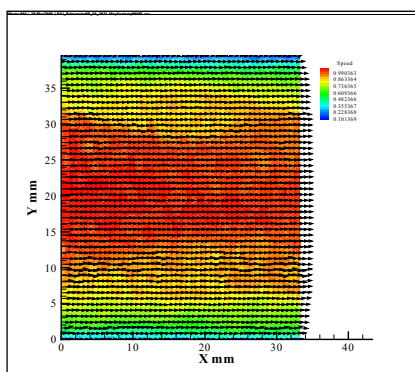


Fig. 9d. $Re=42000$

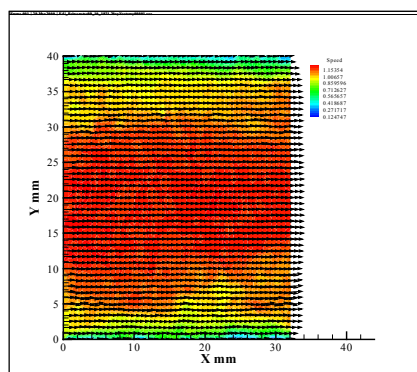


Fig. 9e. $Re=52000$

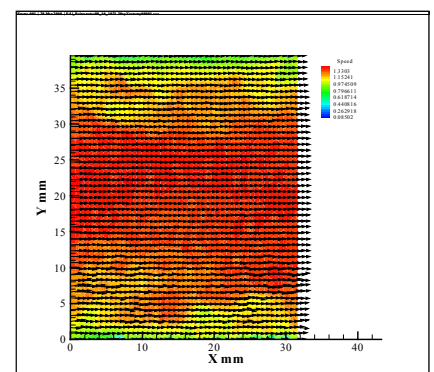


Fig. 9f. $Re=62000$

Fig. 9. Reynolds number dependency of drag reducing flow (CTAC 40ppm)

the figures covers the full channel height. the upper and lower limits of the figure shows the top and bottom surfaces of the channel respectively. The main flow direction is from left to right

disappears. An intermittent change of flow such as turbulent slug was not observed in present study.

2. The instantaneous velocity distribution taken in water flow exhibits the penetration from low speed fluid into high-speed region, which is one of the important events of turbulence energy production and turbulent mixing. Although this structure is commonly observed in water flow, it was not found in drag-reducing flow under the same Reynolds number. The strong vorticity fluctuation near the wall also disappears in drag-reducing flow.
3. As the Reynolds number increases and enters into "post DR region" where Reynolds number exceeds critical value, the drag-reducing flow starts to be unstable and the PIV picture shows an appearance of turbulent motion near the wall.

REFERENCES

- Bewersdorff, H.-W. and Ohlendorf, D.**, (1988). "The Behavior of Drag-Reducing Cationic Surfactant Solutions", *J. Colloid and Polymer Science*, Vol. 266, No. 10, pp941-953.
- Blackwelder, R.F. and Kaplan, R.E.**, (1976). "On the wall structure of the Turbulent Boundary Layer", *J. Fluid Mech.*, 76-1, p89.
- Burger, E.D., Munk, W.R. and Wahl, H.A.**, (1982). "Flow Increase in the Trans-Alaska Pipeline Through Use of a Polymeric Drag-Reduction Additive", *J. Pet. Tech.*, pp.377-386.
- Dean R.B.**, (1978). "Reynolds Number Dependency of Skin Friction and Other Bulk Flow Variables in Two-Dimensional Rectangular Duct Flow", *ASME J. Fluid Eng.*, 100, pp.215-223.
- Gasljevic, K. and Matthys, E.F.**, (1996). "Field Test of a Drag-Reducing Surfactant Additives in a Hydraulic Cooling System", *ASME FED-Vol. 237*, pp. 249-260.
- Gyr, A. and Bewersdorff, H.-W.**, (1995). "Drag Reduction of Turbulent Flows by Additives", Kluwer Academic Publishers, The Netherlands.
- Johansson, A.V. and Alfredsson, P.H.**, (1982). "On the Structure of Turbulent Channel Flow", *J. Fluid Mech.*, 122, pp.295-314.
- Kawaguchi, Y., Yano, T. and Suzuki, K.**, (1983). "'An Experimental Study on Coherent Structure in a Turbulent Boundary Layer Disturbed by a Cylinder", *Proc. 8th Biennial Symp. on Turbulence*, Rolla, MO. USA, 1983.
- Kawaguchi, Y., Tawaraya, Y., Yabe, A., Hishida, K. and Maeda, M.**, (1996a). "Turbulent Transport Mechanism in a Drag Reducing Flow with Surfactant Additive Investigated by Two Component LDV", *8th Intl. Symp. on Appl. of Laser Techniques to Fluid Mechanics*, July 8-11, Lisbon Portugal, II, 29.4.1-29.4.7.
- Kawaguchi, Y., Tawaraya, Y., Yabe, A., Hishida, K. and Maeda, M.**, (1996b). "Active Control of Turbulent Drag Reduction in Surfactant Solutions by Wall Heating", *ASME 1996 Fluid Eng. Div. Conference*, July 7-11, San Diego, USA, Vol.2, pp.47-52.
- Kawaguchi, Y., Daisaka, H., Yabe, A., Hishida, K. and Maeda, M.**, (1997a). "Existence of Double Diffusivity Fluid Layers and Heat Transfer Characteristics in Drag Reducing Channel Flow", in "*Turbulence, Heat and Mass Transfer*", Delft Univ. Press, *Proc. 2nd Intl. Symp. on Turbulence Heat and Mass Transfer*, Delft, The Netherlands, pp.157-166.
- Kawaguchi, Y., Daisaka, H., Yabe, A., Hishida, K. and Maeda, M.**, (1997b). "Turbulence Characteristics in Transition Region of Dilute Surfactant Drag Reducing Flows", *Proc. 11th Intl. Symp. Turbulent Shear Flows*, Sep. Grenoble, France, P1-49-P1-54.
- Li, P.W., Kawaguchi, Y. and Yabe, A.**, (2000). "Feasibility Study of New Heat Transportation System with Drag-reducing Surfactant Additives", *Proc. Symp. on energy Eng. in the 21th Century*, Jan. 9-13, HongKong, China, pp.716-722.
- Mysels, K.J.**, (1949). "Flow of Thickened Fluids", U.S. Patent 2,492,173, December 27.
- Ohlendorf, D., Interthal, W. and Hoffmann, H.**, (1986). "Surfactant Systems for Drag Reduction: Physico-Chemical Properties and Rheological behavior", *Rheol. Acta*, Vol.25, pp.468-486.
- Pollert, J., Zakin, J.L., Myska, J. and Kratochivil, P.**, (1994). "Use of Friction Reducing Additives in District Heating System Field Test at Kladno-Krocehlavy, Czech Republic", *Proc. 85th Int. District Heating and Cooling Assoc.* Seattle, USA, pp.141-156.
- Toms, B.A.**, (1948). "Some Observation on the Flow of Linear Polymer Solutions Through Straight Tubes at Large Reynolds Numbers", *Proc. 1st Intl. Congr. on Rheology*, Vol. II, pp135-141, North Holland, Amsterdam.